Regulatory function of ten-eleven translocation-2 in transcriptional mechanisms of demethylated myeloma cells

LENKA SLAVICKOVA[1], MICHAELA NEMCOVA[1], DOMINIKA SVEHLOVA[1], VERONIKA FRYBORTOVA[1], JIRINA MANAKOVA[2], EVA KRIEGOVA[2], JIRI MINARIK[3,4] and KATERINA SMESNY TRTKOVA[1,5,6]

[1]Department of Clinical and Molecular Pathology, Faculty of Medicine and Dentistry, Palacky University Olomouc, 775 15 Olomouc, Czech Republic; [2]Department of Immunology, Faculty of Medicine and Dentistry, Palacky University Olomouc, 775 15 Olomouc, Czech Republic; [3]Department of Hemato-Oncology, University Hospital Olomouc, 779 00 Olomouc, Czech Republic; [4]Department of Hemato-Oncology, Faculty of Medicine and Dentistry, Palacky University Olomouc, 775 15 Olomouc, Czech Republic; [5]Department of Clinical and Molecular Pathology and Medical Genetics, Faculty of Medicine, University of Ostrava-Zabreh, 703 00 Ostrava, Czech Republic; [6]Department of Clinical and Molecular Pathology and Medical Genetics, Faculty Hospital Ostrava-Poruba, 708 52 Ostrava-Poruba, Czech Republic

Received December 2, 2025; Accepted April 29, 2026

DOI: 10.3892/mmr.2026.13947

Abstract. Multiple myeloma (MM) is a malignant plasma cell disorder characterized by clonal expansion of plasma cells in bone marrow. Genetic aberrations in MM are well-established, while epigenetic alterations, particularly DNA methylation, are increasingly recognized as key regulators of gene expression. The modified bases 5-methylcytosine (5-mC) and 5-hydroxymethylcytosine (5-hmC) occur in gene promoters and regulatory regions. While the presence of 5-mC in the promoter is associated with transcriptional silencing, 5-hmC, generated by oxidation of 5-mC through ten-eleven translocation (TET), is associated with gene activation. The present study investigated promoter-specific 5-hmC and 5-mC levels in *TET1*, *TET2* and *TET3* genes in patients with MM and myeloma cell lines. Quantification of methylation was performed using a glucosylation and enzyme digestion-based method, bisulfite sequencing and nanopore sequencing. *TET* mRNA expression levels were assessed using reverse transcription-quantitative PCR and interactions with specificity protein (Sp)-1 Sp1 and Sp3 transcription factors were analyzed using chromatin immunoprecipitation. *TET* promoter-wide 5-mC and 5-hmC profiles were compared in CD138$^+$ sorted cells from newly diagnosed and relapsed patients with MM and in five myeloma cell lines treated with 5-azacytidine and/or 5-aza-2'-deoxycytidine. In newly diagnosed patients, *TET1* mRNA expression levels were increased in comparison with *TET2* and *TET3*, which corresponded to a reduced CCGG site methylation of the *TET1* promoter (5-10%) and increased *TET3* methylation (21-50%). Of the MM cell lines, the 5-azacytidine-treated KMS12-PE cell line exhibited significantly higher *TET2* gene expression levels when compared with *TET1* and *TET3*. Subsequently, immunoprecipitation with Sp3 demonstrated increased *TET2* recruitment, which suggested a potential interaction between Sp3 and TET2. The present findings indicated dynamic regulation of *TET* genes through CCGG site methylation and hydroxymethylation of their promoter in MM and demonstrated that demethylating agents selectively modulate *TET* gene expression and promoter occupancy, highlighting their potential impact on epigenetic gene activation. Notably, the divergent expression patterns observed suggest that *TET1* acts as an oncogenic driver, while the inducible response of *TET2* highlights its role as a potential tumor suppressor in myeloma biology. Consequently, the present results provide a rationale for the pharmacological restoration of *TET2* expression as a strategic approach to suppress tumor progression through epigenetic reprogramming.

Correspondence to: Dr Katerina Smesny Trtkova, Department of Clinical and Molecular Pathology, Faculty of Medicine and Dentistry, Palacky University Olomouc, 3 Hnevotinska, 775 15 Olomouc, Czech Republic
E-mail: katerina.smesny@upol.cz

Key words: ten-eleven translocation genes, multiple myeloma, demethylation, demethylating agents, specificity protein transcription factors

Introduction

Multiple myeloma (MM) is a malignancy of terminally differentiated plasma cells that accumulate in the bone marrow (BM) (1). Epigenetic remodeling, particularly DNA methylation changes, serves a key role in B-cell differentiation and plasma cell maturation (2). Early B-cell stages are characterized by enhancer demethylation and the upregulation of B-cell transcription factors (TFs). By contrast, late differentiation leads to extensive demethylation of heterochromatin and methylation at Polycomb-repressed genes (3,4). Aberrant retention of methylation patterns has been observed in MM, suggesting a pathogenic role for DNA methylation in disease initiation and progression (5-7).

The therapeutic landscape of MM has been influenced by proteasome inhibitors and immunomodulatory drugs, which have markedly improved patient outcomes (8). Among them, bortezomib is a first-in-class proteasome inhibitor that exerts its antimyeloma effects not only through proteasome blockade but also through induction of reactive oxygen species, intracellular stress, apoptosis and modulation of transcriptional pathways, such as limiting the activity of MYC (9-11). Notably, bortezomib induces microRNA-29b in MM cells and acute myeloid leukemia (AML) cells, leading to downregulation of specificity protein (Sp)-1 and Sp1-regulated genes (12-14). Sp1 and its homolog Sp3 are ubiquitously expressed TFs that bind GC (GGGGCGGGG) boxes to regulate genes controlling differentiation, proliferation and oncogenesis (15). Generally, Sp1 is a transcription activator (16) and Sp3 has been shown to positively regulate transcription (17), but Sp3 can also act as a repressor (18,19). Their upregulation has been associated with poor prognosis in a number of types of solid cancer, such as gastric, pancreatic, colorectal and breast cancer as well as gliomas and squamous cell carcinomas, but their role in MM remains insufficiently characterized (20-24).

DNA methylation dynamics are controlled by ten-eleven translocation (*TET*) methylcytosine dioxygenases, which catalyze the conversion of 5-methylcytosine (5-mC) to 5-hydroxymethylcytosine (5-hmC) and subsequent derivatives, thereby promoting active demethylation (25). The family of *TET* dioxygenases consist of *TET1*, *TET2* and *TET3* (26,27). Previous studies have highlighted the complex epigenomic landscape in MM characterized by notable alterations in cytosine modifications. While global DNA hypomethylation typically occurs during disease progression, hypermethylation contributes to the silencing of tumor suppressor genes (such as *p16*, E-Cadherin and *DAPK*) and non-coding RNAs, such as miR-15 and miR-16 (28-30). Beyond the well-characterized 5-mC, emerging evidence has emphasized the role of 5-hmC, a dynamic intermediate in DNA demethylation catalyzed by *TET* proteins (31,32). In MM, global 5-hmC levels are markedly reduced compared with normal plasma cells. This reduction in 5-hmC is associated with increased disease severity, poor prognosis and inferior overall survival (OS). Furthermore, the distribution of 5-hmC-modified genes in circulating cell-free DNA has been shown to differ depending on patient ancestry, suggesting that *TET*-mediated pathways may contribute to the biological heterogeneity of the disease (33). *TET2* mutations are founder mutations, defined as early clonal events that initiate malignant transformation and are shared by all cells within the tumor clone, in 40-50% of cases of *TET2*-mutant hematopoietic malignancies, while *TET1* and *TET3* partially compensate for *TET2* activity and may constitute potential strategies to treat *TET2* mutated hematopoietic malignancies, including reverting the methylation state of *TET2* target genes (such as *Klf4*, *Jun*, *Chd7* and *Smad3*) (34,35). Despite extensive studies regarding DNA methylation and transcriptional regulation in MM, analyses of *TET* genes in association with Sp1/Sp3 binding and response to demethylating agents remain limited (28,30).

The present study therefore aimed to investigate the interplay between DNA methylation and *TET* gene expression in patients with MM and in MM cell lines. Specifically, the aim was to assess whether demethylating agents can promote Sp1/Sp3 binding to *TET* gene promoters and thereby modulate their expression, uncovering potential epigenetic vulnerabilities in MM.

Materials and methods

Patients with MM. Diagnosis of MM followed the International Myeloma Working Group (IMWG) criteria (36). The present study was approved by the Ethics Committee of University Hospital and the Faculty of Medicine, Palacky University in Olomouc (Olomouc, Czech Republic; approval no. EK FNOL 112/17) and samples were collected following informed consent from the patients.

Patients were eligible for inclusion if they met the following criteria: i) Signed informed consent; ii) age ≥18 years; iii) diagnosis of plasma cell disorder determined according to IMWG criteria, including newly diagnosed MM, relapsed/progressive MM or MM in remission; and iv) availability of BM aspirate suitable for $CD138^+$ plasma cell isolation. A patient with amyloidosis was also included for comparative purposes, as amyloidosis represents an associated plasma cell dyscrasia and was used to complement the spectrum of *TET* mRNA expression profiles across plasma cell disorders (Table I; Fig. 1). Exclusion criteria comprised insufficient quantity or quality of the BM sample, low plasma cell infiltration preventing reliable $CD138^+$ cell sorting or degraded nucleic acids not suitable for downstream analyses.

The $CD138^+$ sorted cell population data was prepared from the plasma cells of BM-aspirate, from 24 patients with MM in different stages: i) Active MM, comprising newly diagnosed patients and patients in relapse/progression as per IMWG criteria; and ii) remission phase MM, defined as achieving at least a partial response after finished initial treatment or being in stable remission after stem cell transplant with continued maintenance therapy. The patients were recruited for the present study at the Department of Hemato-Oncology, University Hospital Olomouc (Olomouc, Czech Republic) between August 2018 and November 2019. All experiments involving patient samples were performed at the Department of Immunology and the Department of Clinical and Molecular Pathology, both within the Faculty of Medicine and Dentistry, Palacky University Olomouc (Olomouc, Czech Republic). The clinicopathological characteristics of the entire cohort (n=24) are provided in Table II.

Among the 24 patients (mean age 64±6 years), 3 patients [two with monoclonal gammopathy of undetermined significance (MGUS) and one newly diagnosed MM] were female and the remaining 21 patients were male. For the quantification of DNA methylation (5-mC and 5-hmC) at a specific CCGG site, a subset of four patients (samples W01-W04) was selected from the primary cohort. The selection was based on the availability of sufficient amounts of high-quality genomic DNA and the requirement to include representative samples from distinct disease stages (newly diagnosed MM, remission and relapse). As a result, the final subset consisted exclusively of male patients, as the available samples from female patients did not meet the quality and/or quantity requirements for this restriction enzyme-based assay. The clinicopathological characteristics of these 4 patients are presented in Table SI.

Table I. No. of patient samples analyzed for each assay across disease stages, stratified by clinical stage.

Analysis	MGUS, n	MM newly diagnosed, n	MM remission, n	MM relapsed, n	Amyloid	Total, n	Male, n	Female, n
Schematic overview of the mRNA expression of *TET* genes	3	16	1	3	1	24	21	3
mRNA expression profiles of *TET* genes	0	16	0	3	0	19	18	1
5-mC in CCGG sites of *TET* genes	0	14	0	3	0	17	16	1
Proportion of 5-mC and 5-hmC in *TET* gene promoters	0	2 (W03 and W04)	1 (W01)	1 (W02)	0	4	4	0

TET, ten-eleven translocation; MM, multiple myeloma; MGUS, monoclonal gammopathy of undetermined significance; 5-mC, 5-methylcytosine; 5-hmC, 5-hydroxymethylcytosine; amyloid, amyloidosis.

A

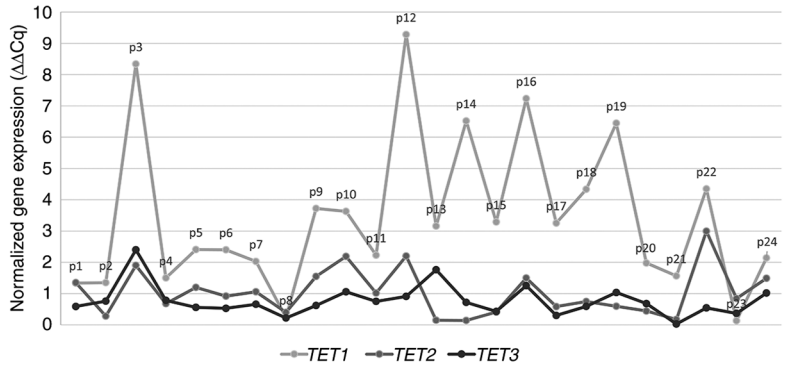

B

		TET1	TET2	TET3
MGUS	p1	1.340 ± 0.07	1.35 ± 0.04	0.590 ± 0.02
MGUS	p2	1.350 ± 0.05	0.280 ± 0.02	0.760 ± 0.15
MGUS	p3	8.340 ± 0.26	1.900 ± 0.11	2.400 ± 0.06
MMdg (W03)	p4	1.501 ± 0.40	0.681 ± 0.00	0.780 ± 0.20
MMdg	p5	2.410 ± 0.06	1.200 ±0.04	0.560 ± 0.02
MMdg	p6	2.400 ± 0.38	0.920 ± 0.02	0.530 ± 0.10
MMdg	p7	2.030 ± 0.01	1.060 ± 0.50	0.660 ± 0.14
MMdg	p8	0.240 ± 0.03	0.400 ± 0.06	0.220 ± 0.30
MMdg	p9	3.720 ± 0.14	1.550 ± 0.25	0.620 ± 0.05
MMdg	p10	3.630 ± 0.40	2.190 ± 0.03	1.060 ± 0.04
MMdg	p11	2.230 ± 0.18	1.020±0.40	0.750 ± 0.02
MMdg	p12	9.280 ± 0.31	2.200 ±0.10	0.910 ± 0.04
MMdg	p13	3.160 ± 0.02	0.150 ± 0.14	1.760 ± 0.00
MMdg	p14	6.520 ± 0.58	0.140 ± 0.40	0.720 ± 0.05
MMdg	p15	3.290 ± 0.31	0.410 ± 0.27	0.430 ± 0.20
MMdg	p16	7.236 ± 0.40	1.497 ± 0.08	1.254 ± 0.15
MMdg	p17	3.256 ± 0.14	0.586 ± 0.36	0.302 ± 0.05
MMdg	p18	4.337 ± 0.25	0.749 ± 0.06	0.593 ± 0.01
MMdg	p19	6.446 ± 0.18	0.597 ± 0.30	1.037 ± 0.45
MMrel (W02)	p20	1.979 ± 0.40	0.446 ± 0.20	0.682 ± 0.02
MMrel	p21	1.556 ± 0.07	0.714 ± 0.04	0.031 ± 0.03
Mmrel	p22	4.349 ± 0.38	2.995 ± 0.02	0.545 ± 0.15
Mmremis (W01)	p23	0.135 ± 0.08	0.843 ± 0.03	0.369 ± 0.04
Amyloid	p24	2.140 ± 0.42	1.490 ± 0.01	1.020 ± 0.16

Figure 1. Schematic overview of the mRNA expression profile of *TET1*, *TET2* and *TET3* genes in CD138$^+$ purified plasma cells obtained from patients in different stages of MM. Individuals are grouped as follows: MGUS stage, patients 1-3; MMdg, patients 4-19; MMrel, patients 20-22; MMremis, patient 23; and patients with amyloidosis, patient 24. (A) Relative mRNA expression levels of *TET1*, *TET2* and *TET3* as determined by reverse transcription-quantitative PCR. mRNA expression was normalized to the β2-microglobulin reference gene. (B) Table showing mean ± SD values of *TET1*, *TET2* and *TET3* mRNA expression levels for each patient. Each patient sample was measured in technical replicate and mean values were used for analysis. TET, ten-eleven translocation; MM, multiple myeloma; MGUS, monoclonal gammopathy of undetermined significance; MMdg, newly diagnosed patients with MM; MMrel, patients with MM in the relapsed stage; MMremis, MM patient in remission.

MM cell lines. In total, 5 different MM cell lines were used: RPMI8226, U266/B1, OPM-2, KMS12-PE and KMS12-BM. The cell lines RPMI8226 (cat. no. CCL155), U266/B1 (cat. no. TIB-196) and OPM-2 (cat. no. ACC 50) were purchased from the American Type Culture Collection and KMS12-BM (cat. no. JCRB0429) and KMS12-PE (cat. no. JCRB0430) cell lines were obtained from the Japanese Cancer Research Resources Bank (National Institute of Biomedical Innovation). To determine their authenticity, the KMS12-BM and KMS12-PE cell lines were assessed using the AmpF/STR™ IdentiFiler™ (Thermo Fisher Scientific, Inc.) for eight short tandem repeat markers in DNA (Tables SII and SIII). The cells were maintained in RPMI-1640 medium supplemented with 10% or 15% FBS, respectively, 1% penicillin-streptomycin antibiotics, 1% L-glutamine and 100 mM sodium pyruvate, at 37˚C with 5% CO_2. Under these conditions, cell lines were treated with 0.2 and 0.5 μmol/l 5-azacytidine (AZA) and/or 5-aza-2'-deoxycytidine (decitabine; DAC) for 48 h with 24 h of re-treatment. Cells treated with an equivalent concentration of DMSO served as vehicle control. All cell line experiments were conducted at the Department of Clinical and Molecular Pathology, Faculty of Medicine and Dentistry, Palacky University Olomouc (Olomouc, Czech Republic).

Reverse transcription-quantitative PCR (RT-qPCR). RNA preparation was performed from CD138$^+$-enriched BM cells using the Single Cell RNA Purification Kit (Norgen Biotek Corp.) and from treated MM cell lines with TRI Reagent® BD (Molecular Research Center, Inc.). Reverse transcription of 100 ng of total RNA was performed using the Transcriptor First Strand cDNA Synthesis Kit (Roche Diagnostics), according to the manufacturer's protocol.

RT-qPCR was conducted with Taq-Man™ probes (cat. no. 4331182; Thermo Fisher Scientific) and Xceed qPCR Probe Mix (cat. no. NPCR 10502 S; Xceed; iBioTech), using the Light cycler® 480 System (Roche Diagnostics). The thermocycling conditions were as follows: Initial denaturation at 95˚C for 10 min, followed by 45 cycles of denaturation

Table II. Clinicopathological characteristics of 24 patients included in the present study.

Characteristics	MGUS (n=3)	MMdg (n=16)	MMrel (n=3)	MMremis (n=1)	Amyloid (n=1)
Sex, n (%)					
Male	1 (33.3)	15 (93.8)	3 (100.0)	1 (100.0)	1 (100.0)
Female	2 (66.7)	1 (6.2)	0 (0.0)	0 (0.0)	0 (0.0)
Age, years	75±7	65±12	77±5	66	53
High-risk cytogenetics, n (%)					
Yes	0 (0.0)	4 (25.0)	2 (66.7)	0 (0.0)	1 (100.0)
No	3 (100.0)	7 (43.8)	0 (0.0)	1 (100.0)	0 (0.0)
Unknown	0 (0.0)	5 (31.2)	1 (33.3)	0 (0.0)	0 (0.0)
Monoclonal immunoglobulin types, n (%)					
IgG	2 (66.7)	14 (87.5)	2 (66.7)	1 (100.0)	0 (0.0)
IgA	1 (33.3)	2 (12.5)	1 (33.3)	0 (0.0)	1 (100.0)
Stage ISS, n (%)					
1		4 (25.0)	0 (0.0)	0 (0.0)	1 (100.0)
2		8 (50.0)	1 (33.3)	0 (0.0)	0 (0.0)
3		3 (18.8)	2 (66.7)	1 (100.0)	0 (0.0)
Unknown		1 (6.2)	0 (0.0)	0 (0.0)	0 (0.0)
Treatment exposure, n (%)					
Untreated	3 (100.0)	0 (0.0)	0 (0.0)	0 (0.0)	0 (0.0)
Proteasome inhibitor based	0 (0.0)	15 (93.8)	1 (33.3)	0 (0.0)	1 (100.0)
IMiD-based (Thal/Len/Pom)	0 (0.0)	7 (43.8)	2 (66.7)	1 (100.0)	0 (0.0)
Anti-CD38 monoclonal antibody	0 (0)	0 (0)	0 (0)	1 (100)	0 (0)
ASCT (transplantation)	0 (0)	1 (6.2)	0 (0)	0 (0)	0 (0)

MM, multiple myeloma; MGUS, monoclonal gammopathy of undetermined significance; MMdg, newly diagnosed patients with MM; MMrel, patients with MM in the relapsed stage; MMremis, MM patient in remission; amyloid, amyloidosis; ISS, International Staging System; IMiD, immunomodulatory imide drugs; Thal, thalidomide; Len, lenalidomide; Pom, pomalidomide; ASCT, autologous stem cell transplantation.

at 95˚C for 15 sec and a combined annealing/extension step at 60˚C for 60 sec.

The mRNA expression levels of *TET1* (assay ID: Hs04189344 g1), *TET2* (assay ID: Hs00766782_s1) and *TET3* (assay ID: Hs00896441_m1) were quantified by RT-qPCR from complementary DNA (cDNA) synthesized by reverse transcription of mRNA and normalized to the expression of endogenous housekeeping control β2-microglobulin (assay ID: Hs00984230_m1). All used probes were provided by Thermo Fisher Scientific, Inc. qPCR data were analyzed using the $2^{-\Delta\Delta Cq}$ quantification method (37), with untreated cells used as the control group.

The human *TET1* transcript NM_030625 is located on chromosome 10 (GRCh38/hg38 assembly) at positions 68560337-68694487 on the plus strand. The promoter region was operationally defined as 1 kb upstream and 1 kb downstream of the transcription start site (TSS). The *TET2* transcript NM_017628.4 is located on chromosome 4 (GRCh38/hg38 assembly) at positions 105145875-105242771 on the plus strand, with the promoter defined at TSS ± 1 kb. The *TET3* transcript NM_001287491.2 is located on chromosome 2 (GRCh38/hg38 assembly) at positions 73984910-74108176 on the plus strand and its promoter was similarly defined relative to TSS.

Western blotting. KMS12-PE and KMS12-BM cell lines were treated with the DNA demethylating agents AZA or DAC at final concentrations of 0.2 and 0.5 μmol/l for 48 h, with retreatment after 24 h. Cells treated with an equivalent concentration of DMSO served as vehicle control.

Total protein lysates were prepared using self-prepared RIPA lysis buffer (10 mM Tris-HCl pH 8.0, 1 mM EDTA, 0.5 EGTA, 140 mM NaCl, 1% Triton X-100, 0.1% sodium deoxycholate and 0.1% SDS) supplemented with protease inhibitors (Roche cOmplete™ Protease Inhibitor Cocktail Tablets; cat. no. 04693124001; Roche Diagnostics). Cells were incubated on ice for 30 min with occasional vortexing and lysates were clarified by centrifugation at 14,000 x g for 15 min at 4˚C. Protein concentration was determined using the Bradford assay (Bio-Rad Protein Assay Dye Reagent Concentrate; cat. no. 5000006; Bio-Rad Laboratories, Inc.).

Equal amounts of protein (20 μg per lane) were mixed with Laemmli sample buffer, boiled at 95˚C for 5 min and resolved by SDS-PAGE on precast 4-15% gradient polyacrylamide gels (Mini-PROTEAN® TGX™; cat. no. 4561085; Bio-Rad Laboratories, Inc.). The use of gradient gels allowed efficient separation of proteins across a broad range of molecular weights (*TET1* ~235 kDa, *TET2* ~130 kDa and

GAPDH ~37 kDa). Electrophoresis was performed at 100 V for ~120 min. Proteins were transferred onto nitrocellulose membranes using semi-dry transfer conditions (10 A for 50 min). The membranes were subsequently cut according to molecular weight and processed separately for incubation with the indicated antibodies. Membranes were then blocked in 5% non-fat dry milk in TBS-T (TBS containing 0.1% Tween-20) for 60 min at room temperature.

For detection of *TET1*, membranes were incubated with rabbit polyclonal anti-*TET1* antibody (cat. no. ab191698; Abcam) diluted 1:1,000 in 5% milk/TBS-T overnight at 4˚C. For detection of *TET2*, membranes were incubated with rabbit polyclonal anti-*TET2* antibody (cat. no. 21207-1-AP; Proteintech Group, Inc.) diluted 1:1,000 in 5% milk/TBS-T overnight at 4˚C.

After primary antibody incubation, membranes were washed 3 times in TBS-T and incubated with HRP-conjugated goat anti-rabbit IgG secondary antibody (cat. no. 7074S; Cell Signaling Technology, Inc.; 1:3,000) for detection of *TET1* and *TET2* or with HRP-conjugated goat anti-mouse IgG secondary antibody (cat. no. 7076S; Cell Signaling Technology, Inc.; 1:5,000) for detection of GAPDH, both for 1 h at room temperature. Following additional washing steps, immunoreactive bands were visualized using the infrared LI-COR Odyssey Imaging System (LI-COR Biosciences) and analyzed using Image Studio software (version 2.0; LI-COR Biosciences). The expected molecular weights were ~235 kDa for *TET1* and 130 kDa for *TET2*. GAPDH was used as a loading control.

Western blotting signals were evaluated qualitatively based on band intensity. Densitometric analysis was not performed, as the experiments were intended to provide supportive determination of expression changes observed at the mRNA level.

Isolation of genomic DNA and detection of 5-hmC in MM cell line. Genomic DNA was isolated from the KMS12-PE cell line using the Wizard® Genomic DNA Purification Kit (Promega Corporation) according to the manufacturer's instructions. DNA concentration and purity were assessed using a NanoDrop™ spectrophotometer (Thermo Fisher Scientific, Inc.) and samples were stored at -20˚C. The isolated genomic DNA was used for colorimetric quantification of global 5-hmC using the MethylFlash™ Hydroxymethylated DNA 5-hmC Quantification Kit (Colorimetric; cat. no. P-1036; EpigenTek Group, Inc.). This assay is based on an ELISA-like format that specifically detects 5-hmC without cross-reactivity to 5-mC or unmodified cytosine.

Genomic DNA (200 nm per well) was bound to the light-affinity strip wells provided in the kit. After DNA binding and washing, a primary capture antibody (cat. no. P-1036-96; EpigenTek Group, Inc.; 1,1000) specific for 5-hmC and a corresponding detection antibody (cat. no. P-1036-48; EpigenTek Group, Inc.; 1:1,000), both provided within the MethylFlash™ Hydroxymethylated DNA 5-hmC Quantification Kit (Colorimetric; cat. no. P-1036; EpigenTek Group, Inc.), were applied according to the manufacturer's instructions. A colorimetric signal was generated using the enhancer and developer solutions, and the absorbance was read at 450 nm on microplate spectrophotometer to obtain optical density (OD) values.

Each sample was measured in triplicate, together with kit-provided negative and positive controls. A calibration curve was generated from the positive control dilution series according to the manufacturer's instructions to allow absolute quantification of 5-hmC. The amount of 5-hmC (ng) in each sample was calculated using the standard curve slope generated from linear regression and the global percentage of 5-hmC relative to input DNA was determined as follows: 5-hmC (ng)=(sample OD450-negative control OD450)/slope x5* and [5-hmC (%)=5-hmC (ng)/S] x100, whereby 'S' refers to the amount of input sample DNA (ng) and '5*' is a factor to normalize 5-hmC in the positive control to 100%, as the positive control contains only 20% of 5-hmC.

Restriction enzyme-based DNA methylation analysis. Both 5-hmC and 5-mC levels at a particular CCGG site were measured with a restriction enzyme-based assay, the EpiMark 5-hmC and 5-mC analysis kit (EpigenTek Group, Inc.) (26,38), according to the manufacturer's instructions. The assay is based on the differential susceptibility of methylated and hydroxymethylated DNA to cleavage by *Hpa*II and *Msp*I. Genomic DNA (620 ng) was treated with 30 units of T4 β-glucosyltransferase and 80 μl uridine diphosphate-glucose at 37˚C for 16 h. Glucosylated DNA was digested with 100 units of *Msp*I, 50 units of *Hpa*II or no enzyme (mock digestion) at 37˚C for 4 h, followed by treatment with 1 μl proteinase K (20 mg/ml) at 40˚C for 30 min.

For qPCR, 1 μl glycosylated/digested DNA was used with promoter-specific primers. Primer sequences were as follows: *TET1* gl (-528): Forward (F), 5'-ACTCCCTGAGGTCTGTCC TG-3' and reverse (R), 5'-CAGGTAGGGCTGCATGACTT-3'; *TET2* gl (-421) F, 5'-GAAGGTGGGCCGGGGCGG-3' and R, 5'-GAGAGGGTGTGCTGCTGAAT-3'; and *TET3* gl (-816) F, 5'-AAAGGCCATGGTAGGAAGTG-3' and R, 5'-TGAAGT AGCGCTGTCCAGAA-3'.

Pyrosequencing™ methylation analysis of CpG sites. Genomic DNA was isolated from BM aspirates and $CD138^+$ sorted cells of patients with MM using a QIAamp DNA Mini Kit (Qiagen GmbH). Bisulfite treatment of extracted genomic DNA was conducted as aforementioned. PCR primers and subsequent pyrosequencing reaction were designed using PyroMark® Assay Design SW 2.0 (Qiagen GmbH). Pyrosequencing primers were designed to the promoter regions of the *TET1* (genomic reference: NC_000010.11, -528 bp upstream of the TSS), *TET2* (genomic reference: NC_000004.12, -421 bp upstream) and *TET3* (genomic reference: NC_000002.12, -816 bp upstream). The primer sequences used were as aforementioned.

In brief, 1 μl bisulfite-treated DNA was added to a 25 μl PCR reaction mixture containing 12.5 μl 1X PyroMark PCR Master Mix (Qiagen GmbH), 1 μl 25 mM $MgCl_2$, 2.5 μl 1X CoralLoad Concentrate (Qiagen GmbH), 0.2 μl forward primer and 0.2 μl biotinylated reverse primer. For HotStartTaq Polymerase activation, the PCR reaction mixture was initially denatured at 95˚C for 15 min, followed by 45 cycles of denaturation at 94˚C for 30 sec, annealing at 56˚C for 30 sec, elongation at 72˚C for 30 sec and the final extension at 72˚C for an additional 10 min after the last cycle. The PCR products were verified by electrophoresis on a 2% agarose gel.

Table III. Representative example of default values for percentage calculation of 5-mC and 5-hmC at 175 bp promoter *TET1*, 236 bp promoter *TET2* and 160 bp promoter *TET3* regions in the W02 sample of $CD138^+$ sort cell population of relapsing patients with MM.

Sample	Target	Reference Cq value	Target/reference Cq value	Normalized ΔΔCq value
W02 *TET1*	Control	29.947 M2	30.547 M1	1.00
W02	Control	29.782 H2	29.943 H1	0.74/hmC
W02	Control	29.609 C2	30.780 C1	1.49/hmC + mC
W02 *TET2*	Control	24.937 M2	25.323 M1	1.00
W02	Control	27.234 H2	27.976 H1	1.28/hmC
W02	Control	25.542 C2	26.365 C1	1.35/hmC + mC
W02 *TET3*	Control	31.739 M2	33.292 M1	1.00
W02	Control	35.747 H2	35.339 H1	0.26/hmC
W02	Control	30.509 C2	32.291 C1	1.17/hmC + mC

M2 (5-hmC), normalized Cq values as target unknown, Tube 1; H2 (5-mC + 5-hmC), normalized Cq values as target unknown, Tube 2; C2, normalized Cq values as target poscalibrator, Tube 3; M1, normalized Cq values as reference unknown, Tube 4; H1, normalized Cq values as reference unknown, Tube 5; C1-normalized Cq values as reference poscalibrator, Tube 6. TET, ten-eleven translocation; MM, multiple myeloma; 5-mC, 5-methylcytosine; 5-hmC, 5-hydroxymethylcytosine.

The incurred biotinylated PCR product was immobilized on Streptavidin Sepharose® High Performance (GE Healthcare), precipitated with 70% ethanol, passed through a denaturation step and then a washing step using PyroMark Q96 Vacuum Workstation (Qiagen GmbH). The amplicons were transferred to each well of the PyroMark Q96 plate containing 40 μl of 0.4 μM sequencing primer diluted in annealing buffer (Qiagen GmbH). Control samples (bisulfite unmethylated and methylated DNA; Qiagen GmbH) were part of a set of analyzed samples from patients with MM. The pyrosequencing analysis was performed using the PyroMark CpG software (version 1.0.11; Qiagen GmbH). The methylation value was quantified in terms of the methylation level (MtL) as the mean percentage of cytosines methylated per CpG: MtL (%)=(Σ% methylated cytosines)/no. of CpGs analyzed.

Quantification of DNA methylation of 5-mc and 5-hmC at a specific CCGG site. To identify DNA methylation changes associated with MM pathogenesis, the 5-mC/5-hmC percentage abundance was investigated in patients at three different stages of MM: i) Newly diagnosed MM (samples W03 and W04); ii) MM in remission (sample W01); and iii) MM in the relapsed stage (sample W02). Calculation of the methylation status of inner C in CCGG sites was performed using the following formula: $C^{hm}CGG$ (%)=[M2 x (C1/C2)]-M1]/C1 and $C^{m}CGG$ (%)=[H1-M2 x (C1/C2)]/C1. Representative values used for these calculations are shown in Table III.

In the calculations (Table SI), the parameters were: M2 (5-hmC), normalized Cq values as target unknown, Tube 1; H2 (5-mC + 5-hmC), normalized Cq values as target unknown, Tube 2; C2, normalized Cq values as target poscalibrator, Tube 3; M1, normalized Cq values as reference unknown, Tube 4; H1, normalized Cq values as reference unknown, Tube 5; C1-normalized Cq values as reference poscalibrator, Tube 6.

The percentages of 5-hmC, 5-mC and cytosine were calculated using the comparative Cq method (Table III) when the *Hpa*II- and *Msp*I-resistant fraction was normalized to the mock digestion control (C2 and C1). The 5-hmC levels were determined directly from the fraction resistant to *Msp*I digestion (M1 and M2), as *Msp*I is inhibited by the presence of 5-hmC but cleaves both unmethylated cytosine and 5-mC. The 5-mC (H2 and H1) levels were obtained by subtracting the 5-hmC contribution from the total *Hpa*II resistance.

Library preparation and nanopore sequencing. Genomic DNA was extracted from the KMS12-PE cell line after the AZA and/or DAC (0.2 and 0.5 μmol/l) treatments using the QIAGEN Blood and Cell Culture DNA Kit (Qiagen GmbH) following the manufacturer's protocol. DNA quality and concentration were assessed using a Qubit® Fluorometer (Invitrogen; Thermo Fisher Scientific, Inc.). Sequencing libraries were prepared using the Oxford Nanopore Technologies Native Barcoding Kit 96 V14 (cat. no. SQK-NBD114.96; Oxford Nanopore Technologies plc) and VAHTS TGS DNA Library Prep Kit for (Vazyme Biotech Co., Ltd.) following the manufacturer's protocol with modifications, including omission of intermediate clean-up steps and adjustment of input DNA and reaction volumes as specified below. The DNA input used was 1,000 ng per sample and end-repair and barcode ligation were performed without intermediate clean-up. After barcode ligation, 2 μl EDTA was added to each sample to stop the reaction prior to pooling. Samples were then pooled and cleaned using AMPure XP beads (cat. no. A63880; Beckman Coulter, Inc.). Adapter ligation was performed using Oxford Nanopore Technologies reagents. DNA concentration was measured with the Qubit® dsDNA HS Assay Kit (Thermo Fisher Scientific, Inc.) and adjusted as needed. For sequencing, 5 μl of the library was included in a final loading mix with total volume 32 μl, which was loaded onto an R10.4.1 flow cell (FLO-PRO114) and sequenced on the PromethION platform (Oxford Nanopore Technologies plc).

Basecalling and 5-mC methylation calling in a CpG context were performed using the Dorado basecaller within the wf-human-variation pipeline (version 2.6.0; Oxford Nanopore Technologies plc). Reads were aligned to the GRCh38 human reference genome using the minimap2 software (version 2.24; Heng Li, Dana-Farber Cancer Institute) and methylation frequencies were generated using the modkit software (version 0.3.3; Oxford Nanopore Technologies plc) with default probability thresholds. Basic quality control was performed to determine high data integrity with a median mapping accuracy of 99%, a read N50 of 39.3 kb and mean sequencing coverage of 4.05x across targeted regions. Analysis of methylation levels was specifically focused on standardized promoter regions of the *TET1, TET2* and *TET3* genes (chromosome 10: 68570336-68595336, chromosome 4: 105105874-105319803 and chromosome 2: 73943630-74175498). Amplicons were designed to cover these coordinates. Methylation levels were calculated per CpG site and summarized for each promoter region, following the coordinates presented in Table SIV.

Chromatin immunoprecipitation (ChIP) and ChIP-qPCR assays. ChIP assays were performed using the Magna ChIP® A/G Chromatin Immunoprecipitation Kit (cat. no. 17-10085; Merck KGaA) according to the manufacturer's instructions. Sonicated chromatin prepared from KMS12-PE cells ($5x10^6$ cell equivalents per immunoprecipitation) was incubated overnight at 4˚C with gentle rotation with 2 μg anti-SP1 (cat. no. ab13370; Abcam) or anti-SP3 (cat. no. ab227856; Abcam) antibodies (diluted in a total volume of 515 μl). Normal rabbit IgG (cat. no. 2729S; Cell Signaling Technology, Inc.; 2 μg) was used as a negative control under the same conditions. Immunoprecipitated DNA was purified using the Magna ChIP® A/G Chromatin Immunoprecipitation Kit (cat. no. 17-10085; Merck KGaA) according to the manufacturer's instructions and subsequently analyzed by qPCR. The ChIP-qPCR conditions were identical to those described above for RT-qPCR. Primers specific for the promoter regions of *TET1* (genomic reference: NC_000010.11; -528 bp upstream of TSS), *TET2* (genomic reference: NC_000004.12; -421 bp upstream) and *TET3* (genomic reference: NC_000002.12; -816 bp upstream) were used for ChIP-qPCR. The primer sequences used for ChIP-qPCR were as aforementioned. The two methods used for ChIP-qPCR data normalization were fold enrichment and percent of input. Fold enrichment is a signal-to-noise ratio comparing the amount of target sequence measured in the immunoprecipitate isolate to the amount measured in a negative control isolate (39). The percent input method compares the amount of target sequence measured in the immunoprecipitate isolate to the total amount of the target sequence in the input isolate (40).

Statistical analysis. Statistical analysis was performed using Statistica software (version 14.0.0.15; TIBCO Software, Inc.). Data are expressed as the mean ± SD. Patient samples were analyzed in technical triplicates and MM cell lines experiments were performed in both biological and technical triplicates. Due to the small sample size and limited number of biological replicates, non-parametric statistical methods were applied. Differences between groups were evaluated using the Kruskal-Wallis test followed by Bonferroni post hoc tests for pairwise comparisons. $P<0.05$ was considered to indicate a statistically significant difference and the adjusted significance level after Bonferroni correction was set at $P<0.005$.

Results

mRNA expression and DNA methylation profiles of TET genes in sorted plasma cells. In the $CD138^+$ sorted plasma cells of both newly diagnosed and relapsed patients with MM, *TET1* mRNA expression levels were increased when compared with that of *TET2* and *TET3* (Figs. 1 and 2A). By contrast, quantitative bisulfite pyrosequencing of the $CD138^+$ purified plasma cell samples showed a decrease in DNA methylation level at *TET1* and *TET2* selected promoter regions in both newly diagnosed and relapsed patients with MM (Table SI), while increased levels of DNA methylation at the *TET3* gene promoter were determined using the pyrosequencing method (Fig. 2B).

TET mRNA expression in demethylated myeloma cell lines. Changes in the mRNA expression levels of *TET* genes after treatment with both demethylating agents was determined in all myeloma lines used, depending on the demethylation agents (AZA and/or DAC) and concentration (0.2 μmol/l and/or 0.5 μmol/l; Fig. 3). For both the KMS12-BM and KMS12-PE cell lines, demethylation treatment altered the normalized *TET2* mRNA expression levels; however, a statistically significant difference between *TET1*, *TET2* and *TET3* expression was observed only in the KMS12-PE cell line ($P<0.001$). The mRNA levels of all three *TET* genes in the U266/B1, RPMI and OMP2 cell lines were found not to be significantly different (Fig. S1). A further demethylation experiment with KMS12-BM and KMS12-PE cell lines validated the results of the increased normalized *TET2* mRNA levels compared with the mRNA expression values of *TET1* and *TET3* (Fig. 3). Increased normalized *TET2* mRNA levels in KMS12-BM did not exhibit a statistical difference. In the KMS12-PE cell line, the normalized value of *TET2* mRNA (5.146±0.29) was evaluated as significantly increased after 0.2 μmol/l AZA treatment compared with normalized *TET1* (1.321±0.16; $P<0.01$) and *TET3* (1.005±0.19; $P<0.05$) mRNA expression levels (Fig. 3).

Western blotting analysis of TET1 and TET2 enzymes. To evaluate the impact of AZA and DAC on the epigenetic regulatory machinery in the KMS12-PE and KMS12-BM cell lines, the protein expression levels of *TET1* and *TET2* were examined using western blotting analysis. Total protein lysate analysis revealed distinct bands at the expected molecular weights for both *TET1* and *TET2*. Visual inspection of the blots revealed that *TET1* protein levels remained stable and did not show an increase following treatment with either AZA or DAC (0.2 and 0.5 μmol/l). By contrast, a marked and consistent increase in TET2 band intensity was observed across all treatment conditions in the KMS12-PE cell line compared with the DMSO control. Representative blots demonstrating these changes are presented in Fig. 3 and repetitive gel experiments demonstrating these findings are provided in Fig. S2. In addition, the original uncropped gels with molecular weight markers are provided in Fig. S3.

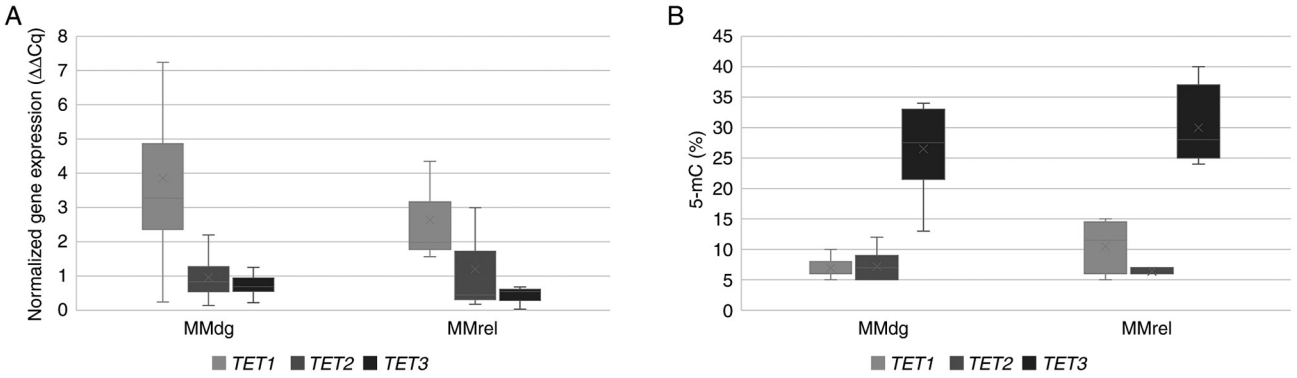

Figure 2. Comparison of *TET1*, *TET2* and *TET3* mRNA expression profiles and levels of CCGG site methylation. (A) mRNA expression profiles of *TET1*, *TET2* and *TET3* genes. (B) Percentage of 5-mC in CCGG sites of their promoter regions. The CD138$^+$ purified plasma cell samples were compared between MMdg and MMrel patients. Regarding mRNA expression levels, n=19 independent patients with MM (MMdg, n=16; MMrel, n=3). For CCGG site methylation levels, n=17 independent patients with MM (MMdg, n=14; MMrel, n=3). Each patient sample was measured in technical replicate and mean values were used for analysis. 5-mC, 5-methylcytosine; TET, ten-eleven translocation; MM, multiple myeloma; MGUS, monoclonal gammopathy of undetermined significance; MMdg, newly diagnosed patients with MM; MMrel, patients with MM in the relapsed stage; MMremis, MM patient in remission.

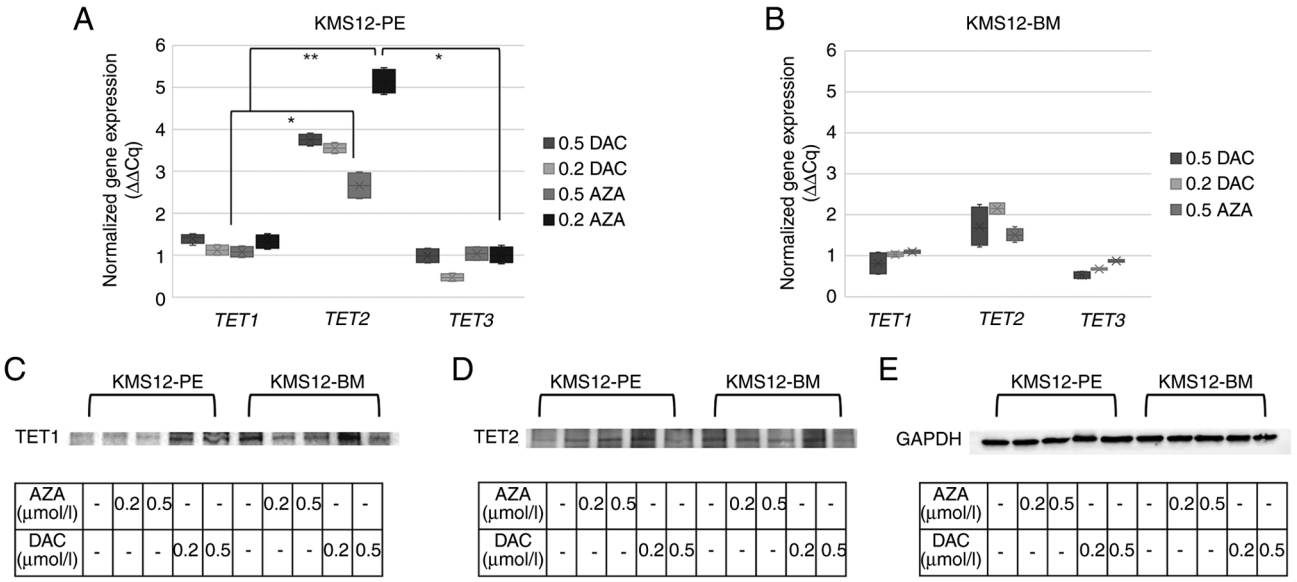

Figure 3. Effect of demethylating agents on *TET* mRNA and protein expression in KMS12-PE and KMS12-BM myeloma cell lines. Comparison of ΔΔCq values of the normalized *TET* mRNA expressions between KMS12-PE and KMS12-BM myeloma cell lines after treatment with demethylating agents. The ΔΔCq value was normalized to DMSO control, using β2-microglobulin as the reference gene, for (A) KMS12-PE and (B) KMS12-BM myeloma cell lines after treatment with AZA (0.2 and 0.5 μmol/l) and/or DAC (0.2 and 0.5 μmol/l) for 48 h, with retreatment after 24 h (n=3 independent biological experiments). Each biological experiment was measured in technical triplicate and mean values were used for analysis. Data are presented as the mean ± SD. The significance was assessed using the Kruskal-Wallis test with Bonferroni correction for pairwise comparisons. *P<0.05 and adjusted P<0.0125; **P<0.01 and adjusted P<0.0025. Western blotting analysis of *TET1* and *TET2* protein expression in KMS12-PE and KMS12-BM cell lines. Representative blots showing the protein levels of (C) TET1 (~235 kDa) and (D) TET2 (~130 kDa) in KMS12-PE and KMS12-BM cells. Cells were treated with indicated concentrations (0.2 and 0.5 μmol/l) of AZA and DAC. (E) GAPDH (37 kDa) was used as a loading control to ensure equal protein loading across all lanes. Proteins were transferred to the same membrane, which was subsequently cut according to molecular weight and probed with the indicated antibodies. TET, ten-eleven translocation; AZA, 5-azacytidine; DAC, 5-aza-2'-deoxycytidine.

Changes in global 5-hmC in the KMS12-PE cell line. Changes in the percentage representation of 5-hmC were evaluated in the KMS12-PE cell line following treatment with demethylating agents AZA (0.2 and 0.5 μmol/l) and DAC (0.2 and 0.5 μmol/l). The percentage of 5-hmC increased from 0.15% in the DMSO control to 0.29 and 0.26% after treatment with AZA at 0.2 and 0.5 μmol/l, respectively and to 0.39 and 0.63% after treatment with DAC at 0.2 and 0.5 μmol/l (Fig. 4). Statistically significant differences in 5-hmC levels were observed across all tested groups (DMSO control, AZA 0.2/0.5 μmol/l and DAC 0.2/0.5 μmol/l; Kruskal-Wallis: P=0.01) and treatment with 0.5 μmol/l DAC differed significantly from the DMSO control (Dunn's test with Bonferroni correction: α=0.005).

5-mC/5-hmC proportion in patients with MM. To further investigate the increased *TET1* mRNA expression levels and the levels of CCGG site methylation of *TET3* promoter in both the newly diagnosed patients with MM and in relapsed stage (Fig. 1), CCGG site methylation patterns of selected promoter *TET* regions in CD138$^+$ purified plasma cells of newly

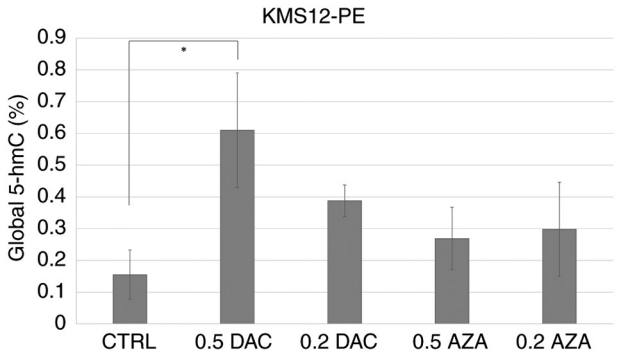

Figure 4. Detection of 5-hmC in the KMS12-PE cell line. Experiments were performed in independent biological and technical replicates. Data are presented as the mean ± SD. The significance was assessed using the Kruskal-Wallis test with Bonferroni correction for pairwise comparisons. *P<0.05 and adjusted P<0.005. 5-hmC, 5-hydroxymethylcytosine; AZA, 5-azacytidine; DAC, 5-aza-2'-deoxycytidine.

diagnosed patients with MM (samples W03 and W04), MM patient in remission (sample W01) and MM patient in relapsed stage (sample W02) were investigated.

The adequacy of the dissociation curves shown in Fig. 5 was determined by highly specific and reproducible melting profiles. Each panel displays overlapping curves from replicates, demonstrating a specific PCR product. Since 5-mC and 5-hmC share the same DNA sequence, they possess identical melting temperatures and thus produce a single dissociation profile per locus. This specificity ensured reliable Cq determination for the enzymatic digestion-based qPCR used to calculate the relative percentages of 5-mC and 5-hmC.

In the newly diagnosed patients with MM, the *TET1* promoter region contained 4.98% (W03) and 7.33% (W04) values of 5-mC without the presence of 5-hmC; whereas 5-hmC was detected in both patients in remission, W01 (6.64%) and patient in relapsed stage W02 (1.92%). Similarly, in the newly diagnosed patients with MM, the *TET2* promoter showed 3.80% (W03) and 11.31% (W04) 5-mC percentage values and in the *TET3*, increased percentage values 34.93% (W03) and 16.59% (W04) as compared with that of *TET1* were determined. The 5-hmC abundance was not found in samples of the newly diagnosed patients (W03 and W04). For all three *TET1*, *TET2* and *TET3* genes investigated, it was determined that the highest 5-hmC levels were in the patient MM in remission (W01) group: 6.64, 8.29 and 1.49% respectively; while patients in the relapsed stage (W02) showed low levels of 5-hmC: 1.92, 1.63 and 1.70% for *TET1*, *TET2* and *TET3* respectively. In comparison with both W01 and W02 patients, the highest incidence of DNA methylation changes in the promoter of all tested *TET* genes was found in both newly diagnosed patients with MM (W03 and W04; Fig. 5A).

Methylation frequencies (5-mC) of TET genes after demethylation of myeloma cells. Analysis of DNA methylation patterns in the *TET* genes of the KMS12-PE cell line demonstrated a significant reduction in methylation levels in samples treated with demethylating agents compared with that of the untreated control. The control group exhibited a mean methylation frequency ~37% in the *TET1* gene, 41% in *TET2* and 41% in *TET3*, with minimal variability as determined by Nanopore sequencing and methylation calling (Fig. 6B). By contrast, samples treated with AZA and DAC showed markedly decreased methylation levels across all three genes. The methylation frequencies for 0.2 μmol/l AZA were ~20% (*TET1*), 12% (*TET2*) and 20% (*TET3*), while for cells treated with 0.5 μmol/l AZA, the frequencies were 16% (*TET1*), 18% (*TET2*) and 14% (*TET3*), all showing high variability. After treatment with 0.2 μmol/l DAC, the frequency of methylation was ~22% (*TET1*), 14% (*TET2*) and 19% (*TET3*). The percentage of methylation after 0.5 μmol/l DAC treatment was 27% (*TET1*), 8% (*TET2*) and 16% (*TET3*), also with high variability.

Specific binding of Sp1/Sp3 TFs and genes encoding TET enzymes. ChIP analysis was performed with KMS12-PE cells to determine the specific binding of Sp1/Sp3 to the individual promoter sequence of *TET* genes under previously applied demethylation conditions (AZA and/or DAC at concentrations of 0.2 μmol/l and/or 0.5 μmol/l). Fig. 7 shows that Sp1 recruitment to the *TET1* and *TET3* promoters significantly increased following DAC treatment, peaking at 0.2 μmol/l DAC for both. While Sp1 binding to the *TET2* promoter remained low at 0.2 μmol/l DAC, a notable increase was observed at 0.5 μmol/l DAC. In addition, 0.5 μmol/l AZA treatment moderately enhanced Sp1 binding across all three *TET* promoters, whereas the 0.2 μmol/l AZA dose resulted in negligible enrichment.

By contrast to Sp1, Sp3 exhibited a more pronounced response to AZA treatment at the higher concentration (0.5 μmol/l), which resulted in the highest enrichment for both genes *TET2* and *TET3*. DAC treatment led to a slight, dose-dependent increase in Sp3 binding at the TET3 promoter but had minimal impact on *TET2* (Fig. 8).

Discussion

TET gene mRNA expression profiles in CD138$^+$ sorted plasma cells of patients with MM showed an increased mRNA expression level of the *TET1* gene in both newly diagnosed and relapsed patients. However, in previous studies, *TET1* was shown to be downregulated in numerous types of cancer, such as breast cancer, oral squamous cell carcinoma, lymphoma and non-small cell lung carcinoma (7,41-43). By contrast to the frequent downregulation and key tumor suppressor roles of *TET* genes observed in these types of cancer (44), *TET1* is a direct target of mixed-lineage leukemia (MLL) fusion proteins and is markedly upregulated in MLL-rearranged leukemia, leading to a global increase of 5-hmC. Furthermore, while bisulfite pyrosequencing in the present study cohort showed reduced DNA methylation levels of the *TET1* promoter, the increased levels of 5-mC in the *TET3* promoter corresponded to *TET3* reduced mRNA expression. It should be noted that among the 24 patients with MM included in the present study, only three were female (two with MGUS and one newly diagnosed MM), while the remaining patients were male. Due to the small number of female samples, potential sex-specific effects on *TET* expression and methylation could not be assessed.

Lineage continuity and differentiation of hematopoietic stem and progenitor stem cells are regulated by transcriptional programming in interplay with DNA methylation and histone

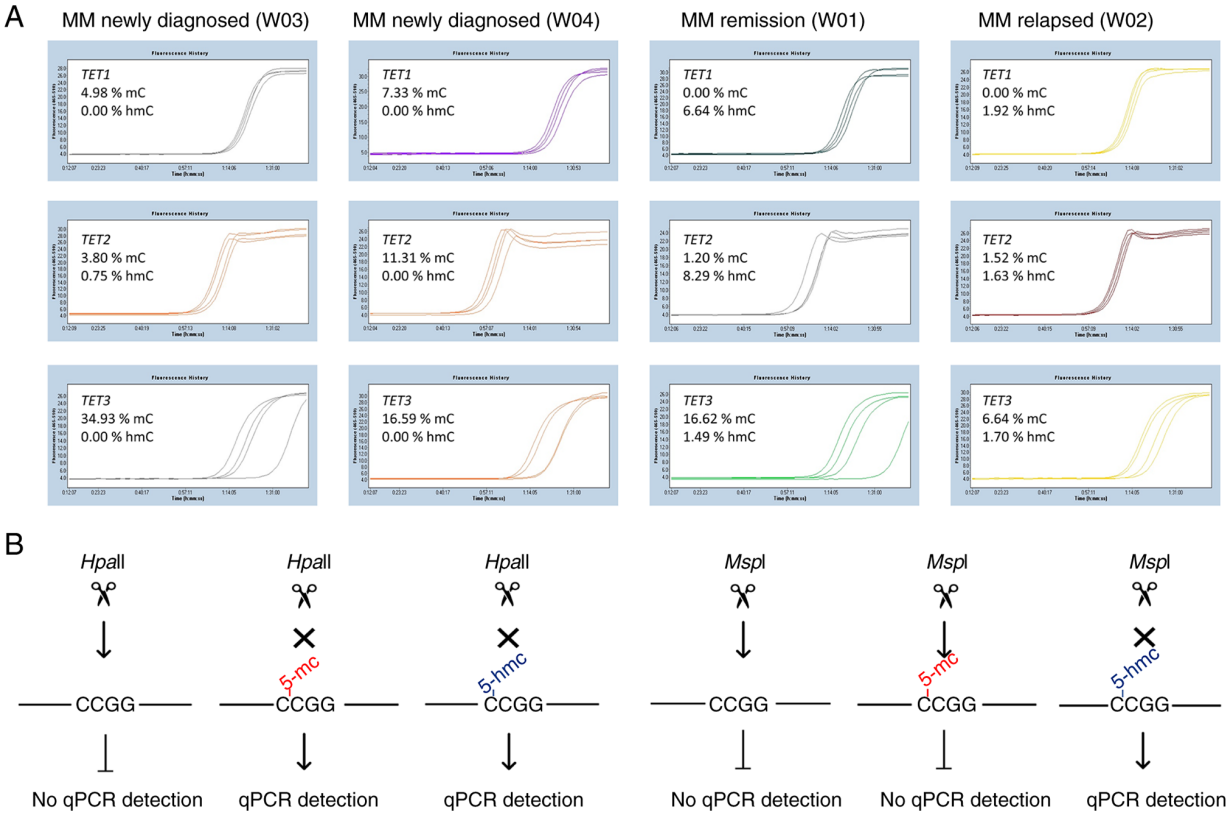

Figure 5. Proportion of 5-mC and 5-hmC in *TET* gene promoters in plasma cells from selected patients with MM from the original cohort. (A) The 5-mC/5-hmC ratio in promoter regions of *TET* genes was analyzed in CD138$^+$ purified plasma cells from newly diagnosed patients with MM (W03 and W04), a patient with MM in remission (W01) and a MM patient in the relapsed stage (W02). Dissociation curves determined the specificity of qPCR amplification for each analyzed *TET* promoter region, showing single melting peaks corresponding to the expected amplicons. Each dissociation curve represents a single qPCR reaction. Further 5-mC and 5-hmC percentages were calculated from Cq values obtained after enzymatic digestion-based qPCR using multiple digestion conditions [n=4 independent patients with MM (W01-W04)]. (B) Schematic representation of the principle of 5-mC and 5-hmC discrimination using *Hpa*II and *Msp*I digestion at CCGG sites within *TET1-3* promoter regions. *Hpa*II cleaves unmethylated CCGG sites but is inhibited by both 5-mC and 5-hmC, resulting in the detection of the combined 5-mC and 5-hmC fraction. *Msp*I cleaves unmethylated and 5-mC sites but is inhibited by 5-hmC, enabling selective detection of 5-mC. 5-mC levels were calculated by subtracting the 5-hmC fraction from the total *Hpa*II-resistant fraction. TET, ten-eleven translocation; MM, multiple myeloma; 5-mC, 5-methylcytosine; 5-hmC, 5-hydroxymethylcytosine; qPCR, quantitative PCR.

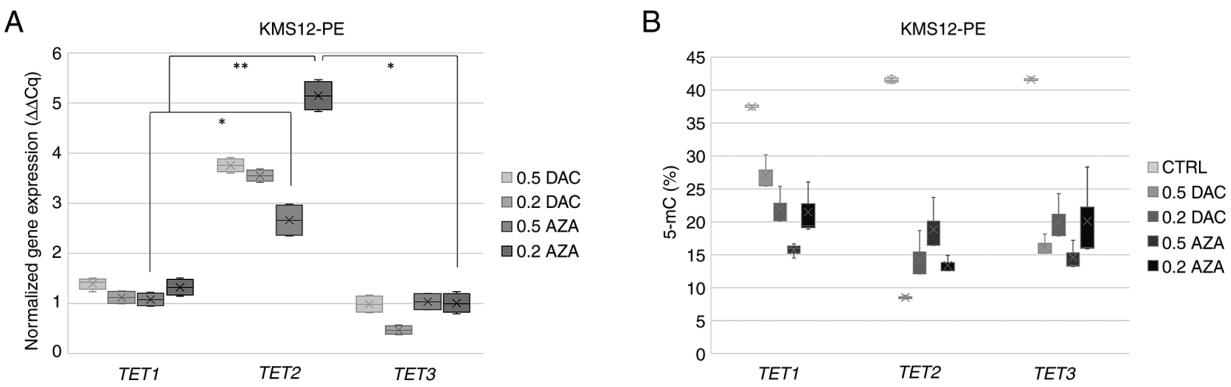

Figure 6. Comparison of *TET* mRNA expression and CCGG site methylation levels in the KMS12-PE cell line. (A) Normalized *TET* mRNA expression (ΔΔCq) in KMS12-PE cell line after treatment with AZA (0.2 and 0.5 μmol/l) and/or (0.2 and 0.5 μmol/l). Cells were treated for 48 h, with retreatment after 24 h. Data are normalized to the DMSO control, with β2-microglobulin used as the reference gene. (B) Percentage of methylation in KMS12-PE myeloma cell lines after treatment with AZA (0.2 and 0.5 μmol/l) and/or DAC (0.2 and 0.5 μmol/l) for 48 h, with retreatment after 24 h. Methylation levels targeting *TET* gene promoter regions were determined by Oxford Nanopore Technologies sequencing. Experiments were performed in independent biological and technical replicates. Data are presented as the mean ± SD. The significance was assessed using the Kruskal-Wallis test with Bonferroni correction for pairwise comparisons. *P<0.05 and adjusted P<0.0125; **P<0.01 and P<0.0025. TET, ten-eleven translocation; MM, multiple myeloma; 5-mC, 5-methylcytosine; MMdg, newly diagnosed patients with MM; AZA, 5-azacytidine; DAC, 5-aza-2'-deoxycytidine; CTRL, control.

modifications (4,35,45). Aberrant DNA methylation patterns have been observed in almost all types of hematopoietic malignancies, including myelodysplastic syndromes, AML, diffuse large B-cell lymphoma and peripheral T-cell

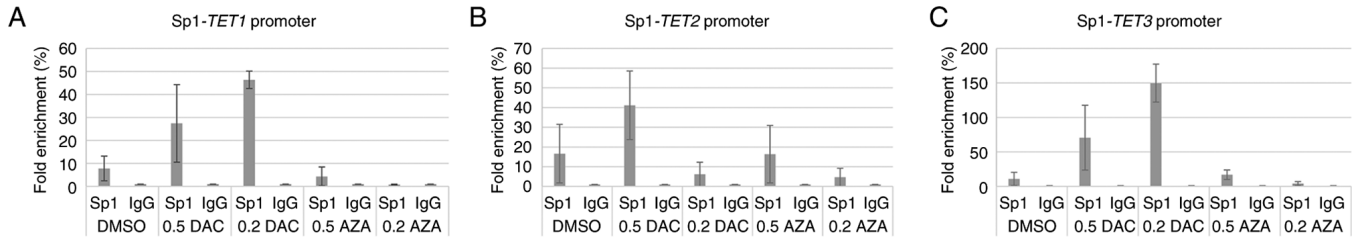

DMSO	Sp1	7.80
	IgG	1.00
0.5 µmol/l DAC	Sp1	27.42
	IgG	1.00
0.2 µmol/l DAC	Sp1	46.36
	IgG	1.00
0.5 µmol/l AZA	Sp1	4.32
	IgG	1.00
0.2 µmol/l AZA	Sp1	0.81
	IgG	1.00

DMSO	Sp1	16.63
	IgG	1.00
0.5 µmol/l DAC	Sp1	41.16
	IgG	1.00
0.2 µmol/l DAC	Sp1	6.15
	IgG	1.00
0.5 µmol/l AZA	Sp1	16.36
	IgG	1.00
0.2 µmol/l AZA	Sp1	1.67
	IgG	4.66

DMSO	Sp1	10.83
	IgG	1.00
0.5 µmol/l DAC	Sp1	70.64
	IgG	1.00
0.2 µmol/l DAC	Sp1	149.74
	IgG	1.00
0.5 µmol/l AZA	Sp1	16.99
	IgG	1.00
0.2 µmol/l AZA	Sp1	4.12
	IgG	1.00

Figure 7. Chromatin immunoprecipitation-quantitative PCR fold enrichment analysis of Sp1 binding to *TET* promoters in KMS12-PE myeloma cells. Enrichment of (A) *TET1*, (B) *TET2* and (C) *TET3* promoter sequences was measured following immunoprecipitation with an anti-Sp1 antibody (n=3 independent biological experiments). Each biological experiment was measured in technical triplicate and mean values were used for analysis. Data are presented as the mean ± SD. TET, ten-eleven translocation; AZA, 5-azacytidine; DAC, 5-aza-2'-deoxycytidine.

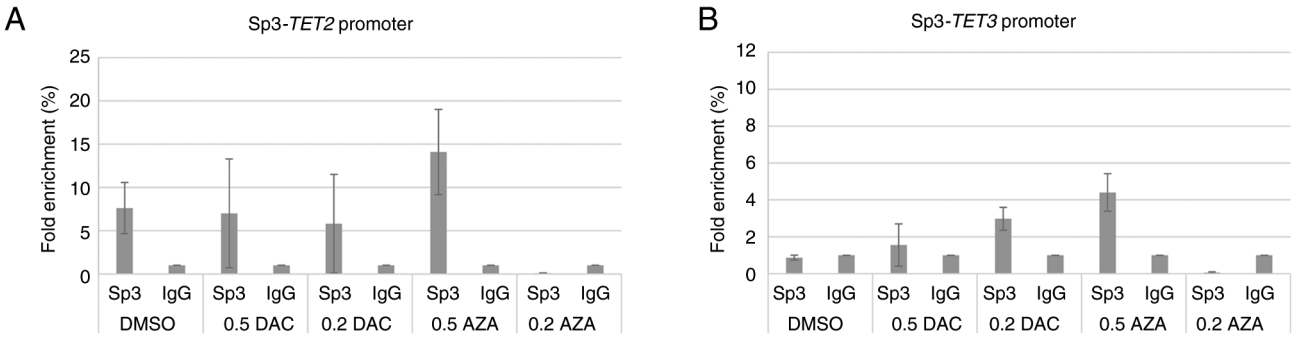

DMSO	Sp3	7.60
	IgG	1.00
0.5 µmol/l DAC	Sp3	7.01
	IgG	1.00
0.2 µmol/l DAC	Sp3	5.81
	IgG	1.00
0.5 µmol/l AZA	Sp3	14.09
	IgG	1.00
0.2 µmol/l AZA	Sp3	0.09
	IgG	1.00

DMSO	Sp3	0.87
	IgG	1.00
0.5 µmol/l DAC	Sp3	1.55
	IgG	1.00
0.2 µmol/l DAC	Sp3	2.97
	IgG	1.00
0.5 µmol/l AZA	Sp3	4.40
	IgG	1.00
0.2 µmol/l AZA	Sp3	0.06
	IgG	1.00

Figure 8. Chromatin immunoprecipitation-quantitative PCR fold enrichment analysis of Sp3 binding to *TET* promoters in KMS12-PE myeloma cells. Enrichment of (A) *TET2* and (B) *TET3* promoter sequences was measured following immunoprecipitation with an anti-Sp3 antibody (n=3 independent biological experiments). Each biological experiment was measured in technical triplicate and mean values were used for analysis. Data are presented as the mean ± SD. TET, ten-eleven translocation; AZA, 5-azacytidine; DAC, 5-aza-2'-deoxycytidine.

lymphoma (46-49). Furthermore, somatic mutations of DNA methylation regulators such as DNA methyltransferase 3A, isocitrate dehydrogenase *(IDH)*-1, *IDH2* and *TET2* further underscore the central role of epigenetic dysregulation of these diseases (50). Therefore, *TET2* could function as a key epigenetic regulator of DNA methylation, as its disruption is associated with a number of hematological malignancies (51,52).

The present study detected significantly increased relative mRNA expression of the *TET2* gene in two myeloma cell lines, KMS12-PE and KMS12-BM. These findings suggested the presence of methylation changes; particularly, the presence of 5-mC in the CG dinucleotides of the promoter region of *TET2* gene, which was reduced by the following demethylation treatment. AZA and DAC treatment led to demethylation in *TET* promoters, which was reflected in changes in mRNA expression levels. Significantly increased mRNA expression levels of *TET2* in demethylated myeloma cell lines suggested the potential of *TET2* expression as a biomarker of the hypomethylation process in association with a good prognosis of MM.

This upregulation was confirmed at the translational level. The present western blotting analysis demonstrated an increase in *TET2* protein expression across all treatment conditions in the KMS12-PE cell line, consistent with the mRNA data. By contrast, *TET1* protein levels remained stable after treatment with demethylating agents.

TET enzymes are directly responsible for the conversion of 5-mC to 5-hmC and increased *TET* expression (26) is therefore expected to be accompanied by elevated 5-hmC levels. Similarly, treatment of KMS12-PE cells with AZA and DAC resulted in an increase in the percentage representation of 5-hmC compared with the DMSO control, with a statistically significant effect observed for 0.5 μmol/l DAC, in the present study. These findings provided functional support for the upregulation of *TET2* expression observed in the present study and suggested that increased *TET2* transcript levels are reflected at the level of DNA hydroxymethylation. However, this analysis was performed in a single MM cell line (KMS12-PE), which was selected as it exhibited the most pronounced increase in *TET2* expression following AZA/DAC treatment and validation in additional MM cell lines and primary patient samples would further strengthen these findings.

The KMS12-PE cell line used in the present study is derived from extramedullary MM (pleural effusion), which represents a biologically distinct form of the disease compared with BM-resident myeloma. This cell line was established alongside KMS12-BM from the same patient, documenting the progression from BM involvement to a more advanced, extramedullary stage (53). Extramedullary myeloma often exhibits distinct biological and therapeutic responses compared with BM disease, potentially due to differences in microenvironmental interactions, genetic and epigenetic profiles and treatment sensitivity. These factors may contribute to the divergent responses to DAC and AZA observed between KMS12-BM and KMS12-PE samples in the present study. Therefore, while KMS12-PE represents a relevant model for advanced and aggressive disease, the findings may not fully capture the complete heterogeneity of MM. Further validation in additional cell lines and primary patient samples is warranted to demonstrate these observations across different disease stages.

The present findings revealed a distinct mRNA expression pattern that aligns with the recently proposed roles of *TET* enzymes in hematological malignancies (54). Specifically, high mRNA expression of *TET1* were observed alongside low mRNA levels of *TET2* in primary patient samples, a phenotype that was reversed upon treatment in cell lines, where *TET2* (but not *TET1*) was significantly upregulated. This inverse association suggested that *TET1* and *TET2* serve opposing roles in disease biology. Consistent with previous studies regarding T-cell acute lymphoblastic leukemia and other hematologic malignancies, TET1 has been implicated as a pro-oncogenic factor associated with tumor maintenance and adverse prognosis, whereas *TET2* acts as a tumor suppressor. Notably, *TET2* is the most frequently mutated TET family member in hematological diseases, with loss-of-function alterations representing early events in disease development, in contrast to the rare mutations observed in *TET1* and *TET3* (55). In MM however, *TET2* mutations are relatively rare (~1% of patients in the Myeloma XI trial), although they have still been identified as early driver events in disease development (8). Notably, increased *TET2* expression has been associated with improved OS in MM, supporting its tumor-suppressive role in this context (56).

Such observations are also consistent with a model described in T-cell acute lymphoblastic leukemia, where *TET1* acts as an oncogene required for tumor maintenance, while *TET2* functions as a potent tumor suppressor whose expression is actively repressed by oncogenic drivers such as MYC (57). By contrast, the role of TET1 in MM remains less clearly defined. Although increased expression of *TET1* has been associated with poor prognosis in certain hematological malignancies, such as MLL-rearranged leukemia and AML, context-dependent effects, including reports of *TET1* hypermethylation, suggest that its function may vary across disease types and remains to be fully elucidated in MM (55).

The reactivation of *TET2* following therapeutic intervention in the present KMS12-PE cell line contrasted with its low baseline in patients, supported the hypothesis that *TET2* represents a key 'therapeutic vulnerability'. Therefore, while high *TET1* levels may serve as a marker of active disease biology and oncogenic maintenance, the inducible response of *TET2* suggests its role as a key mediator of epigenetic reprogramming toward a tumor-suppressive state.

Myelomagenesis is initiated through a pre-malignant state known as MGUS. Aberrant DNA methylations have been observed in almost all disease stages of MM, with the transition from MGUS to MM characterized by genome-wide hypomethylation and gene-specific hypermethylation (8,29). Therefore, epigenetic dysregulation is thought to be involved in the development and progression of plasma cell neoplasms (58) and a decreased percentage value of 5-hmC in patients with MM, which may reflect insufficient demethylation of genes associated with disease progression.

The degree of aberrant DNA methylation may be an important indicator for determining prognosis and selecting treatment for MM. Malignant transformation is typically characterized by a widespread reduction of genomic 5-hmC across various tissue types. This epigenetic mark is generated by TET hydroxylases, which catalyze the conversion of 5-mC to 5-hmC. In line with this biochemical process, tumor samples exhibit a depletion of 5-hmC relative to healthy tissues, with numerous studies having associated diminished 5mhC levels with worse clinical prognosis. Rather than being distributed evenly, this loss of 5-hmC specifically targets genic regions, suggesting the disruption of transcriptionally active chromatin in cancer cells (59,60). The percentage abundance of 5-mC and 5-hmC in $CD138^+$ sorted cells in newly diagnosed patients with MM was evaluated in the present study. This exploratory analysis suggested that 5-mC/5-hmC proportions may be present at different MM stages. In particular, higher 5-hmC levels observed in the remission stage of patients with MM samples may reflect increased demethylation activity, whereas lower 5-hmC levels detected in the relapsed stage sample may be associated with renewed methylation of the *TET* gene promoters. While the presence of 5-mC was observed in these patients, increased percentage abundance of 5-hmC occurred in other stages of MM, including the remission and relapsed stages. However, variations in 5-hmC abundance across disease stages require further validation in larger, stage- and sex-balanced cohorts.

The results of nanopore sequencing demonstrated that treatment with demethylating agents such as AZA and DAC led to a significant reduction in the DNA methylation levels of *TET* genes. In untreated control samples, *TET* genes exhibited high levels of methylation, which were markedly reduced in the samples treated with demethylating agents. The most notable decrease in methylation occurred in the *TET2* gene, which was associated with increased mRNA expression of *TET2*. These findings suggested that both AZA and DAC effectively inhibit DNA methylation in *TET2* gene regions, potentially restoring or altering their epigenetic regulation. This reduction in methylation may lead to increase expression of this gene, which is key for maintaining DNA demethylation and regulating gene expression.

Detection and quantification of DNA methylation and hydroxymethylation remain technically challenging. Common methods, including bisulfite sequencing, pyrosequencing, microarray-based approaches and emerging third-generation sequencing technologies such as single molecule, real-time and Oxford Nanopore Technologies, vary in sensitivity, resolution and applicability to repetitive regions or low-abundance modifications (61,62). While methods such as nanopore sequencing offer single-molecule resolution and the ability to distinguish 5-mC from 5-hmC, genome-wide profiling in clinical samples is still limited by sample size and technical complexity. Furthermore, the present study did not include orthogonal validation of 5-hmC signals using methods such as *TET*-assisted bisulfite sequencing, which represents a limitation and should be considered when interpreting the modification profiles. In the context of MM, these methodological limitations underscore the challenges of studying epigenetic regulation in patient-derived cells. The present findings of altered *TET* gene expression suggested that DNA methylation dynamics may serve a role in the pathogenesis of MM. Unlike genetic mutations, epigenetic modifications are potentially reversible, highlighting DNA methylation and hydroxymethylation as promising therapeutic targets. Enzyme-mediated detection of cytosine derivatives could therefore provide valuable insights into the epigenetic landscape of MM and guide future interventions.

According to the present findings, the demethylation agents, AZA and DAC were associated with increased binding of Sp1/Sp3 TFs to the studied *TET* enzymes in the KMS12-PE cells. For Sp1, occupancy at the *TET1* and *TET3* promoters increased notably following DAC treatment, which suggested that these genes may be primary targets of Sp1 even under conditions of DNA demethylation and be a part of the complex activating the transcription mechanism accompanying tumor cell proliferation. The particularly strong enrichment at *TET3*, reaching up to 149-fold, may indicate that Sp1 binding is highly responsive to DAC and AZA treatment and may be associated with transcriptional activation of this locus. In contrast to the initial assumption of a universal decrease, Sp1 binding at the *TET2* promoter showed a dose-dependent response; specifically, a marked increase was observed after 0.5 μmol/l DAC treatment (reaching a 41.16-fold enrichment). This suggests that Sp1 may actively contribute to the restored *TET2* gene expression following demethylation, acting as a positive regulator of this potential tumor suppressor.

By contrast, the Sp3, as a potential TF of the inactive transcription, displayed a different binding profile. An increase in Sp3 binding was observed at the *TET2* promoter, particularly following 0.5 μmol/l AZA treatment. This recruitment of Sp3 is associated with the previously observed increase in *TET2* expression, suggesting that Sp3, alongside Sp1, may serve a key role in the functional restoration of the TET2 tumor suppressor pathway in KMS12-PE cells. Finally, the present findings indicate differential patterns of Sp1 and Sp3 binding across *TET* gene promoters, perhaps influenced by promoter architecture, chromatin accessibility and cofactor interactions and highlight the need for further studies to clarify their functional impact. However, it is important to note that ChIP-qPCR enrichment solely demonstrates physical occupancy at the promoters and does not inherently prove transcriptional regulation. These results provide a preliminary outline of Sp1/Sp3 involvement, which should be further determined by functional assays, such as Sp1/Sp3 knockdown or luciferase reporter experiments, to demonstrate any causal associations between TF recruitment and *TET* promoter activity.

In summary, the present study provides a promoter-focused view of *TET* gene regulation by combining methylation analysis with Sp1/Sp3 promoter occupancy and cellular response to AZA/DAC treatment. Notably, it was demonstrated that demethylating agents not only upregulate *TET2* expression but are also associated with increased global 5-hmC levels, supporting enhanced catalytic activity. The present results, showing activation of *TET2* upon treatment in comparison to its low baseline expression in patient samples, suggest that *TET2* may function as a tumor suppressor, the repression of which is key in maintaining the malignant phenotype. This contrasts with *TET1*, which appears to act as an oncogenic driver in the active disease state. While the present study primarily addressed epigenetic regulation of *TET* genes, the downstream transcriptional programs associated with *TET2* activation remain to be defined. Elucidating these pathways may further clarify the role of *TET2* in MM biology.

Acknowledgements

The authors would like to thank Mr. Ondrej Brzoň (NGS GEEKS Division, I.T.A.-Intertact s.r.o; Prague, Czech Republic) for their help in evaluating the nanopore sequencing results.

Funding

The present study received financial support from Palacky University Olomouc (grant nos. IGA LF_2024_10 and IGA_LF2023_046), RVO from University Hospital Olomouc (grant no. FNOL, 00098892), the EXCELES programme (grant no. LX22NPO5102), the Czech Ministry of Education (grant no. DRO 61989592) and the Czech Ministry of Health (grant no. DRO FNOl 00098892).

Availability of data and materials

The sequencing data generated in the present study may be found in the NCBI Sequence Read Archive under BioProject accession number PRJNA1465408 or at the following URL: https://www.ncbi.nlm.nih.gov/sra/?term=PRJNA1465408.

Authors' contributions

LS performed the experiments, analyzed the data and wrote the manuscript. MN and VF performed the experiments and analyzed the data. DŠ performed the experiments. JMa performed the clinical experiments and analyzed the clinical data. EK analyzed the clinical data and revised the manuscript. JMi provided patient samples, contributed to the acquisition and interpretation of clinical data and critically revised the manuscript for important intellectual content. KST analyzed the data and wrote the manuscript. LS and KST confirm the authenticity of all the raw data. All authors read and approved the final version of the manuscript.

Ethics approval and consent to participate

The present study was approved by the Ethics Committee of University Hospital Olomouc (Olomouc, Czech Republic; approval no. EK FNOL 112/17). Written informed consent was obtained from the patients for this publication.

Patient consent for publication

Not applicable.

Competing interests

The authors declare that they have no competing interests.

References

1. Rajkumar SV: Multiple myeloma: Every year a new standard? Hematol Oncol 37 (Suppl 1): S62-S65, 2019.
2. Kulis M, Queirós AC, Beekman R and Martín-Subero JI: Intragenic DNA methylation in transcriptional regulation, normal differentiation and cancer. Biochim Biophys Acta 1829: 1161-1174, 2013.
3. Lee ST, Xiao Y, Muench MO, Xiao J, Fomin ME, Wiencke JK, Zheng S, Dou X, de Smith A, Chokkalingam A, *et al*: A global DNA methylation and gene expression analysis of early human B-cell development reveals a demethylation signature and transcription factor network. Nucleic Acids Res 40: 11339-1151, 2012.
4. Kulis M, Merkel A, Heath S, Queirós AC, Schuyler RP, Castellano G, Beekman R, Raineri E, Esteve A, Clot G, *et al*: Whole-genome fingerprint of the DNA methylome during human B cell differentiation. Nat Genet 47: 746-756, 2015.
5. Barwick BG, Powell DR, Penaherrera D, Skerget S, Keats JJ, Auclair D, Lonial S, Boise LH and Vertino PM: Abstract 839: Whole genome DNA methylation analysis of multiple myeloma identifies pervasive hypomethylation and biomarkers of survival. Cancer Res 79 (Suppl 13): S839, 2019.
6. Barwick BG, Scharer CD, Martinez RJ, Price MJ, Wein AN, Haines RR, Bally APR, Kohlmeier JE and Boss JM: B cell activation and plasma cell differentiation are inhibited by de novo DNA methylation. Nat Commun 9: 1900, 2018.
7. Agirre X, Castellano G, Pascual M, Heath S, Kulis M, Segura V, Bergmann A, Esteve A, Merkel A, Raineri E, *et al*: Whole-epigenome analysis in multiple myeloma reveals DNA hypermethylation of B cell-specific enhancers. Genome Res 25: 478-487, 2015.
8. Yang T, Liu X, Kumar SK, Jin F and Dai Y: Decoding DNA methylation in epigenetics of multiple myeloma. Blood Rev 51: 100872, 2022.
9. Maneix L, Iakova P, Moree SE, Hsu JI, Mistry RM, Stossi F, Lulla P, Sun Z, Sahin E, Yellapragada SV and Catic A: Proteasome inhibitors silence oncogenes in multiple myeloma through localized histone deacetylase 3 (HDAC3) stabilization and chromatin condensation. Cancer Res Commun 2: 1693-1710, 2022.
10. Xian M, Cao H, Cao J, Shao X, Zhu D, Zhang N, Huang P, Li W, Yang B, Ying M and He Q: Bortezomib sensitizes human osteosarcoma cells to adriamycin-induced apoptosis through ROS-dependent activation of p-eIF2α/ATF4/CHOP axis. Int J Cancer 141: 1029-1041, 2017.
11. Lipchick BC, Fink EE and Nikiforov MA: Oxidative stress and proteasome inhibitors in multiple myeloma. Pharmacol Res 105: 210-215, 2016.
12. Walker AR, Klisovic RB, Garzon R, Schaaf LJ, Humphries K, Devine SM, Byrd JC, Grever MR, Marcucci G and Blum W: Phase I study of azacitidine and bortezomib in adults with relapsed or refractory acute myeloid leukemia. Leuk Lymphoma 55: 1304-1308, 2014.
13. Amodio N, Di Martino MT, Foresta U, Leone E, Lionetti M, Leotta M, Gullà AM, Pitari MR, Conforti F, Rossi M, *et al*: miR-29b sensitizes multiple myeloma cells to bortezomib-induced apoptosis through the activation of a feedback loop with the transcription factor Sp1. Cell Death Dis 3: e436, 2012.
14. Liu S, Liu Z, Xie Z, Pang J, Yu J, Lehmann E, Huynh L, Vukosavljevic T, Takeki M, Klisovic RB, *et al*: Bortezomib induces DNA hypomethylation and silenced gene transcription by interfering with Sp1/NF-kappaB-dependent DNA methyltransferase activity in acute myeloid leukemia. Blood 111: 2364-2373, 2008.
15. Li L and Davie JR: The role of Sp1 and Sp3 in normal and cancer cell biology. Ann Anat 192: 275-283, 2010.
16. Suske G: The Sp-family of transcription factors. Gene 238: 291-300, 1999.
17. Pagliuca A, Gallo P and Lania L: Differential role for Sp1/Sp3 transcription factors in the regulation of the promoter activity of multiple cyclin-dependent kinase inhibitor genes. J Cell Biochem 76: 360-367, 2000.
18. Ammanamanchi S and Brattain MG: Sp3 is a transcriptional repressor of transforming growth factor-beta receptors. J Biol Chem 276: 3348-3352, 2001.
19. Safe S: Specificity Proteins (Sp) and cancer. Int J Mol Sci 24: 5164, 2023.
20. Wang F, Ma YL, Zhang P, Shen TY, Shi CZ, Yang YZ, Moyer MP, Zhang HZ, Chen HQ, Liang Y and Qin HL: SP1 mediates the link between methylation of the tumour suppressor miR-149 and outcome in colorectal cancer. J Pathol 229: 12-24, 2013.
21. Guan H, Cai J, Zhang N, Wu J, Yuan J, Li J and Li M: Sp1 is upregulated in human glioma, promotes MMP-2-mediated cell invasion, and predicts poor clinical outcome. Int J Cancer 130: 593-601, 2012.
22. Jiang NY, Woda BA, Banner BF, Whalen GF, Dresser KA and Lu D: Sp1, a new biomarker that identifies a subset of aggressive pancreatic ductal adenocarcinoma. Cancer Epidemiol Biomarkers Prev 17: 1648-1652, 2008.
23. Maurer GD, Leupold JH, Schewe DM, Biller T, Kates RE, Hornung HM, Lau-Werner U, Post S and Allgayer H: Analysis of specific transcriptional regulators as early predictors of independent prognostic relevance in resected colorectal cancer. Clin Cancer Res 13: 1123-1132, 2007.
24. Wang L, Wei D, Huang S, Peng Z, Le X, Wu TT, Yao J, Ajani J and Xie K: Transcription factor Sp1 expression is a significant predictor of survival in human gastric cancer. Clin Cancer Res 9: 6371-6380, 2003.
25. Ko M, An J, Pastor WA, Koralov SB, Rajewsky K and Rao A: TET proteins and 5-methylcytosine oxidation in hematological cancers. Immunol Rev 263: 6-21, 2015.
26. Ito S, Shen L, Dai Q, Wu SC, Collins LB, Swenberg JA, He C and Zhang Y: Tet proteins can convert 5-methylcytosine to 5-formylcytosine and 5-carboxylcytosine. Science 333: 1300-1303, 2011.
27. Tahiliani M, Koh KP, Shen Y, Pastor WA, Bandukwala H, Brudno Y, Agarwal S, Iyer LM, Liu DR, Aravind L and Rao A: Conversion of 5-methylcytosine to 5-hydroxymethylcytosine in mammalian DNA by MLL partner TET1. Science 324: 930-935, 2009.
28. Deaton AM and Bird A: CpG islands and the regulation of transcription. Genes Dev 25: 1010-1022, 2011.
29. Walker BA, Wardell CP, Chiecchio L, Smith EM, Boyd KD, Neri A, Davies FE, Ross FM and Morgan GJ: Aberrant global methylation patterns affect the molecular pathogenesis and prognosis of multiple myeloma. Blood 117: 553-562, 2011.
30. Sharma A, Heuck CJ, Fazzari MJ, Mehta J, Singhal S, Greally JM and Verma A: DNA methylation alterations in multiple myeloma as a model for epigenetic changes in cancer. WIREs Syst Biol Med 2: 654-669, 2010.

31. Morey Kinney SR and Pradhan S: Ten Eleven Translocation Enzymes and 5-Hydroxymethylation in mammalian development and cancer. Adv Exp Med Biol 754: 57-83, 2013.
32. Amodio N, D'Aquila P, Passarino G, Tassone P and Bellizzi D: Epigenetic modifications in multiple myeloma: Recent advances on the role of DNA and histone methylation. Expert Opin Ther Targets 21: 91-101, 2017.
33. Mason MJ and Chiu BC: Racial disparities in multiple myeloma: Biological heterogeneity, treatment access, and prognostic implications. Leuk Lymphoma 67: 27-39, 2026.
34. Joshi K, Liu S, Breslin SJP and Zhang J: Mechanisms that regulate the activities of TET proteins. Cell Mol Life Sci 79: 363, 2022.
35. Joshi K, Zhang L, Breslin SJP, Kini AR and Zhang J: Role of TET dioxygenases in the regulation of both normal and pathological hematopoiesis. J Exp Clin Cancer Res 41: 294, 2022.
36. Rajkumar SV: Multiple myeloma: 2022 update on diagnosis, risk stratification, and management. Am J Hematol 97: 1086-1107, 2022.
37. Livak KJ and Schmittgen TD: Analysis of relative gene expression data using real-time quantitative PCR and the 2(-Delta Delta C(T)) method. Methods 25: 402-408, 2001.
38. Kennedy BE, Hundert AS, Goguen D, Weaver IC and Karten B: Presymptomatic alterations in amino acid metabolism and DNA methylation in the cerebellum of a murine model of Niemann-Pick type C disease. Am J Pathol 186: 1582-1597, 2016.
39. Solomon ER, Caldwell KK and Allan AM: A novel method for the normalization of ChIP-qPCR data. MethodsX 8: 101504, 2021.
40. Nagaki K, Talbert PB, Zhong CX, Dawe RK, Henikoff S and Jiang J: Chromatin immunoprecipitation reveals that the 180-bp satellite repeat is the key functional DNA element of Arabidopsis thaliana centromeres. Genetics 163: 1221-1225, 2003.
41. Good CR, Panjarian S, Kelly AD, Madzo J, Patel B, Jelinek J and Issa JJ: TET1-mediated hypomethylation activates oncogenic signaling in triple-negative breast cancer. Cancer Res 78: 4126-4137, 2018.
42. Li L, Li C, Mao H, Du Z, Chan WY, Murray P, Luo B, Chan AT, Mok TS, Chan FK, *et al*: Epigenetic inactivation of the CpG demethylase TET1 as a DNA methylation feedback loop in human cancers. Sci Rep 6: 26591, 2016.
43. Cimmino L, Dawlaty MM, Ndiaye-Lobry D, Yap YS, Bakogianni S, Yu Y, Bhattacharyya S, Shaknovich R, Geng H, Lobry C, *et al*: TET1 is a tumor suppressor of hematopoietic malignancy. Nat Immunol 16: 653-662, 2015.
44. Huang H, Jiang X, Li Z, Li Y, Song CX, He C, Sun M, Chen P, Gurbuxani S, Wang J, *et al*: TET1 plays an essential oncogenic role in MLL-rearranged leukemia. Proc Natl Acad Sci USA 110: 11994-11999, 2013.
45. McKinney-Freeman S, Cahan P, Li H, Lacadie SA, Huang HT, Curran M, Loewer S, Naveiras O, Kathrein KL, Konantz M, *et al*: The transcriptional landscape of hematopoietic stem cell ontogeny. Cell Stem Cell 11: 701-714, 2012.
46. Langemeijer SM, Aslanyan MG and Jansen JH: TET proteins in malignant hematopoiesis. Cell Cycle 8: 4044-4048, 2009.
47. Reddy A, Zhang J, Davis NS, Moffitt AB, Love CL, Waldrop A, Leppa S, Pasanen A, Meriranta L, Karjalainen-Lindsberg ML, *et al*: Genetic and functional drivers of diffuse large B cell lymphoma. Cell 171: 481-494.e15, 2017.
48. Jiang M, Bennani NN and Feldman AL: Lymphoma classification update: T-cell lymphomas, Hodgkin lymphomas, and histiocytic/dendritic cell neoplasms. Expert Rev Hematol 10: 239-249, 2017.
49. Cruz-Rodriguez N, Combita AL and Zabaleta J: Epigenetics in hematological malignancies. Methods Mol Biol 1856: 87-101, 2018.
50. Woods BA and Levine RL: The role of mutations in epigenetic regulators in myeloid malignancies. Immunol Rev 263: 22-35, 2015.
51. Nakajima H and Kunimoto H: TET2 as an epigenetic master regulator for normal and malignant hematopoiesis. Cancer Sci 105: 1093-1099, 2014.
52. Bowman RL and Levine RL: TET2 in normal and malignant hematopoiesis. Cold Spring Harb Perspect Med 7: a026518, 2017.
53. Lio CWJ, Yuita H and Rao A: Dysregulation of the TET family of epigenetic regulators in lymphoid and myeloid malignancies. Blood 134: 1487-1497, 2019.
54. Muylaert C, Van Hemelrijck LA, Maes A, De Veirman K, Menu E, Vanderkerken K and De Bruyne E: Aberrant DNA methylation in multiple myeloma: A major obstacle or an opportunity? Front Oncol 12: 979569, 2022.
55. Pawlyn C, Kaiser MF, Heuck C, Melchor L, Wardell CP, Murison A, Chavan SS, Johnson DC, Begum DB, Dahir NM, *et al*: The spectrum and clinical impact of epigenetic modifier mutations in myeloma. Clin Cancer Res 22: 5783-5794, 2016.
56. Ohtsuki T, Yawata Y, Wada H, Sugihara T, Mori M and Namba M: Two human myeloma cell lines, amylase-producing KMS-12-PE and amylase-non-producing KMS-12-BM, were established from a patient, having the same chromosome marker, t(11;14)(q13;q32). Br J Haematol 73: 199-204, 1989.
57. Poole CJ, Zheng W, Lodh A, Yevtodiyenko A and van Riggelen J: TET1 and TET2 maintain transcriptional profiles of T-ALL cells in a MYC-dependent manner. Cancer Cell Int 19: 184, 2019.
58. Ohya M, Nakazawa K and Kanno H: Lower number of 5-hydroxymethylcytosine-expressing cells in plasma cell myeloma than in reactive plasma cell hyperplasia: A useful immunohistochemical approach for identification of neoplastic plasma cells. Pathology 51: 81-85, 2019.
59. Li W and Xu L: Epigenetic function of TET family, 5-methylcytosine, and 5-hydroxymethylcytosine in hematologic malignancies. Oncol Res Treat 42: 309-317, 2019.
60. Alberge JB, Magrangeas F, Wagner M, Denié S, Guérin-Charbonnel C, Campion L, Attal M, Avet-Loiseau H, Carell T, Moreau P, *et al*: DNA hydroxymethylation is associated with disease severity and persists at enhancers of oncogenic regions in multiple myeloma. Clin Epigenetics 12: 163, 2020.
61. Li Y and Tollefsbol TO: DNA methylation detection: Bisulfite genomic sequencing analysis. Methods Mol Biol 791: 11-21, 2011.
62. Hu T, Chitnis N, Monos D and Dinh A: Next-generation sequencing technologies: An overview. Hum Immunol 82: 801-811, 2021.